Hindawi
Journal of Oncology
Volume 2021, Article ID 2986489, 11 pages
https://doi.org/10.1155/2021/2986489

Research Article

MicroRNA-2355-5p Promotes the Proliferation of Head and Neck Squamous Cell Carcinoma via Suppressing NISCH Expression

Hailin Zhang,[1,2,3] **Wei Xie**,[2,4] **Ying Liu**,[5] **Bocheng Zhang**,[1,2,3] **Mingjing Peng**,[1,2] **Sha Li**,[2,3] **Xiaowu Sheng**,[2] **Huayi Ren**,[6] **Qian Gong**,[6] **Zan Li**,[2,3,7] **Chenhui Luo**,[2] **Jie Dai**,[1,2,3] **Xiao Zhou**,[1,2,3,7] **and Ying Long**[1,2,7]

[1]*Translational Medicine Centre, Hunan Cancer Hospital and the Affiliated Cancer Hospital of Xiangya School of Medicine, Central South University, Changsha, Hunan 410013, China*
[2]*Hunan Provincial Clinical Research Centre for Oncoplastic Surgery, Hunan Cancer Hospital and the Affiliated Cancer Hospital of Xiangya School of Medicine, Central South University, Changsha, Hunan 410013, China*
[3]*Department of Head & Neck Surgery, Hunan Cancer Hospital and the Affiliated Cancer Hospital of Xiangya School of Medicine, Central South University, Changsha, Hunan 410013, China*
[4]*Department of Hepatobiliary Surgery, Hunan Cancer Hospital and the Affiliated Cancer Hospital of Xiangya School of Medicine, Central South University, Changsha, Hunan 410013, China*
[5]*Hunan Traditional Chinese Medical College, Zhuzhou, Hunan 412012, China*
[6]*Department of Pharmacy, Hunan Cancer Hospital and the Affiliated Cancer Hospital of Xiangya School of Medicine, Central South University, Changsha, Hunan 410013, China*
[7]*Hunan Provincial Clinical Research Centre for Wound Rehabilitation, Hunan Cancer Hospital and the Affiliated Cancer Hospital of Xiangya School of Medicine, Central South University, Changsha, Hunan 410013, China*

Correspondence should be addressed to Ying Long; longying@hnca.org.cn

Received 16 August 2021; Accepted 11 October 2021; Published 22 October 2021

Academic Editor: Ashok Pandurangan

Background. MicroRNAs (miRNAs) have emerged as crucial regulators in various cancers. However, the potential role of miR-2355-5p in head and neck squamous cell carcinoma (HNSC) remains unclear. *Methods*. Bioinformatics methods were implemented to find the candidate target gene of miR-2355-5p. Quantitative real-time PCR was performed to detect RNA expression levels of miR-2355-5p and NISCH, while western blot was carried out for the detection of protein levels of NISCH and cell cycle-related biomarkers. CCK-8, EdU staining, and flow cytometry were employed to measure cell proliferation and cell cycle progression. Dual-luciferase assay and RNA pulldown were conducted to verify the binding relationship between miR-2355-5p and NISCH. *Results*. The expression levels of miR-2355-5p and NISCH were, respectively, higher and lower in HNSC tissues than those in normal adjacent tissues. The transfection of the miR-2355-5p inhibitor suppressed cell proliferation by arresting the cells at the G1/S transition. The results of luciferase activity and RNA pulldown assays indicated that miR-2355-5p directly targeted the NISCH 3′-untranslated region. Furthermore, the effects of miR-2355-5p inhibition on cell proliferation were reversed after treatment with siRNA against NISCH. *Conclusion*. In summary, our findings indicate that miR-2355-5p promotes cell cycle progression in HNSC by targeting NISCH. Hence, targeting miR-2355-5p could be a promising therapeutic strategy for the treatment of HNSC

1. Introduction

Head and neck squamous cell carcinoma (HNSC) is the sixth leading incident cancer worldwide, and the occurrence of HNSC has increased over the past decades [1–3]. Despite the relatively low incidence of distant metastasis in HNSC, the outcome of patients remains unsatisfactory in recent years [4]. Tumor cells with uncontrolled proliferation provide them with growth advantages, and consequently produce tumor recurrence after treatment. These cells are always characterized by derangements in the cell cycle regulation [5, 6]. Hence, it is essential to dissect the molecular disorders during the cell cycle regulation of HNSC cells, which might contribute to providing novel therapeutic targets for HNSC treatment.

miRNA is a class of noncoding RNA of approximately 22 nT that regulates gene expression at the post-transcriptional level by binding to the 3′-untranslated region(3′-UTR) of its target, inducing mRNA degradation or translational repression [7, 8]. Accumulating evidence supports the involvement of microRNAs (miRNAs) in the regulation of cell proliferation, apoptosis, invasion, migration, and other phenotypes [9]. Our previous study showed that miR-26b-5p suppresses the proliferation of CAL27 cells through targeting PRR11 [10]. Cheng et al. indicated that miR-2355-5p affects the expression of γ-globin in the thalassaemia patients [11]. Previous studies have demonstrated that the miR-2355 gene plays an important role in the development and progression of various cancers as a key mediator of competing endogenous RNA (ceRNA) axes, including pancreatic cancer, oesophageal squamous cell carcinoma, bladder cancer, and chondrosarcoma [12–15]. Furthermore, miR-2355 expression significantly correlated with the response against platinum-based therapy in cervical, head and neck, and lung cancers [16]. To data, the involvement of miR-2355-5p in HNSC remains unclear. Recently, bioinformatics tools have facilitated an integrative understanding of miRNA functions and their roles in carcinogenesis, metastasis, and chemoresistance by identifying miRNA targets [17–20]. NISCH, the coding gene of Nischarin, was predicted as a candidate target of miR-2355-5p in the current study. Previously, NISCH has been implicated in the regulation of cell cycle progression as a tumor suppressor [21–24]. However, the potential roles of NISCH in HNSC remain unclear.

In the present study, miR-2355-5p was found to be upregulated in HNSC and contributed to the promotion of HNSC cell proliferation. Together with the prediction of the miR-2355-5p binding site within the NISCH 3′-UTR, we hypothesized that miR-2355-5p could promote HNSC cell proliferation via targeting NISCH. Our results shed new light on the mechanism that provides HNSC cells with growth advantages.

2. Materials and Methods

2.1. Tissues and Cell Lines. Twelve pairs of frozen samples were collected from HNSC patients with informed consent from the Hunan Cancer Hospital. All the experiments were approved by the ethics committee of the Hunan Cancer Hospital (KYJJ-2020-222), Changsha, China. HNSC cell lines, CAL27, and SCC25 were purchased from Shanghai Genechem Co. Ltd, and routinely cultured in DMEM with 10% FBS (Gibco, Gaithersburg, MD). Each siRNA, miRNA mimics, or inhibitor (GenePharm, Shanghai, China) was transfected into HNSC cells for 48 hours using Lipofectamine 2000 (Invitrogen, Carlsbad, CA).

2.2. Bioinformatics and Statistical Analysis. The gene expression data (FPKM) of HNSC patients were downloaded from The Cancer Genome Atlas (TCGA; https://cancergenome.nih.gov) [25]. Then, the data of candidate genes were extracted to form a new matrix. Differences in gene expression between groups were assessed using the Student's *t*-test. Programs of microT (20–22) and miRmap (23, 24) were employed for the prediction of candidate targets for miR-2355-5p using the Encyclopedia of RNA Interactomes (ENCORI) online tools [26, 27], followed by the removal of miRNA-target pairs without crosslinking immunoprecipitation (CLIP) or Degradome data. The Pearson correlation coefficient (PCC) value between each pair was subsequently calculated with the TCGA-HNSC data. Only pairs with PCC < -0.2 and corrected p value <0.05 would be considered as statistically significant correlation, and the others were excluded. Candidate genes were then subjected to overall survival (OS) analysis using the univariate Cox regression model with the *R* package survival (CRAN.R-project.org/package = survival, version 2.43–3), and $p < 0.05$ was considered to be statistically significant. The candidate gene whose expression correlated with the OS of TCGA-HNSC patients was considered to be the potential target of miR-2355-5p. The relationship between gene expression and outcome of TCGA-HNSC patients was visualized as Kaplan–Meier plotters using a web tool OncoLnc (http://www.oncolnc.org) [28].

2.3. Quantitative Real-Time PCR (qRT-PCR). The total RNA of each specimen was extracted using the Trizol reagent (Invitrogen, Carlsbad, CA). According to the manufacturer's instructions, the total RNA was then reverse transcribed to cDNA using the PrimeScriptTM RT-PCR Kit (Takara, Dalian, China) for protein-coding gene quantitation and using PrimeScript RT reagent kit (Takara, Dalian, China) with specific stem-loop primers for miRNA quantitation. Quantitative real-time PCR (qRT-PCR) was performed using SYBR® Premix DimerEraser™ (Takara, Dalian, China) in a Roche LightCycler 480 II Real-Time PCR system (Roche, Basel, Switzerland). The threshold cycle value (Ct) of each product was measured and normalized against that of the internal control of GAPDH (for protein-coding gene) or U6 (for miRNA), and the differences were compared by using the *t*-test using SPSS version 23.0, with the statistical significance set at $p < 0.05$.

2.4. Cell Counting Kit-8 (CCK-8) Assay. Each group of cells were seeded into 96-well plates at 2×10^3 cells/well. The CCK-8 (Beyotime, China, C0041) reagent was injected into

the well after 0-, 12-, 24-, 48-, and 72-hour of culturing. Using a microplate reader, the optical density at 450 nm was recorded after a 2-hour incubation.

2.5. Cell Cycle Analysis. For each group of cells, cell cycle analysis was performed by flow cytometry after propidium iodide (PI) staining. Cell pellets (about 1.0×10^6) were washed and suspended in 200 μl of cold PBS and fixed in 4 ml of 70% ethanol overnight at −20°C. All specimens were centrifuged and resuspended in 500 μl of buffer containing 40 μg/ml propidium iodide (Beyotime, China, C1052) and 100 μg/ml RNase A (Beyotime, China, C1052) and incubated for 30 min at 37°C before analysis on a CytoFLEX flow cytometer (Beckman Coulter). Data were analyzed by using the CytExpert (Beckman Coulter, Version 2.0) software.

2.6. EdU Staining. Proliferating cells were stained with EdU (5-ethynyl-2′-deoxyuridine) with the cell-light EdU Apollo567 in vitro kit (RiboBio, Guangzhou, China, C10310). Each group of HNSC cells was seeded and transfected with different molecules for 48 hours. Then, cells were washed twice and stained with 10 μM EdU for 30 min, followed by 4′,6-diamidino-2-phenylindole (DAPI, Thermo, USA, 1306) staining. The plates were finally observed and photographed under a microscope (Olympus, Tokyo, Japan, CX41-72C02) at 200x magnification.

2.7. Dual-Luciferase Reporter Gene Assay. Vectors for luciferase reporter assay were generated based on the pmirGLO dual-luciferase miRNA target expression vector (Promega, Madison, WI), including pmirGLO-NISCH 3′-UTR-wt (wildtype) and pmirGLO-NISCH 3′-UTR-mut (miR-2355-5p binding site mutated). The plasmids were then cotransfected with miR-2355-5p or negative control (NC) mimics into CAL27 cells with lipofectamine 2000, respectively. The relative luciferase activity was measured using the dual-luciferase reporter assay system (Promega, Madison, WI).

2.8. RNA Pulldown. The vectors, pcDNA3.1-NISCH-wt, and pcDNA3.1-NISCH-mut were constructed for the overexpression of NISCH with wildtype 3′-UTR and mutated 3′-UTR. CAL27 cells were transfected with pcDNA3.1-NISCH-wt and pcDNA3.1-NISCH-mut for 48 hours, and then the cell lysates were collected. Biotinylated probes complementary to NISCH mRNA and random probes were synthesized (GenePharm, Shanghai, China). The M-280 streptavidin magnetic beads (Sigma-Aldrich, St. Louis, MO) were coated with these probes. Cell lysates were then incubated with the probe-coated beads at 4°C overnight, and molecules interacting with NISCH mRNA were captured after washing. The bound RNAs were subsequently purified using TRIzol, and the abundance of miR-2355-5p and NISCH was finally measured by qRT-PCR.

2.9. Western Blot. Each group of cells was lysed in RIPE buffer at 4°C for 30 min and centrifuged at 15,000 g for 15 min to obtain the protein sediment. After separation by SDS-polyacrylamide gel electrophoresis (SDS-PAGE) and transferring to PVDF membranes (Millipore, Billerica, MA), the protein specimens were incubated with primary antibodies against NISCH (ProteinTech, IL, USA, 13813, 1 : 1,000 dilution), Cyclin D1 (Bioss, Beijing, China, bs-0623R, 1 : 500 dilution), p-Rb^{Ser807} (abcam, CA, UK, ab131264, 1 : 1,000 dilution), and ß-actin (ProteinTech, IL, USA, 66009, 1 : 2,000 dilution) overnight at 4°C, followed by incubation with the secondary antibody (ProteinTech Group Inc., Chicago, IL, 1 : 6,000 dilution) for 1 h at room temperature. The signals were finally measured with an enhanced chemiluminescence (ECL) kit (Pierce, Rockford, IL).

3. Results

3.1. miR-2355-5p Was Upregulated in HNSC Tissues. Using the data from the TCGA-HNSC dataset, we found that miR-2355-5p was significantly upregulated in HNSC tissues as compared with the normal tongue tissues (Figure 1(a)). The similar expression pattern of miR-2355-5p was subsequently validated between 12 collected HNSC tissues and their matched paracancer tissues by using qRT-PCR (Figure 1(b)). Moreover, the Kaplan–Meier survival curve suggests poor OS with higher expression of miR-2355-5p than those in the low miR-2355-5p expression group (Figure 1(c)).

3.2. NISCH Is a Direct Target of miR-2355-5p in HNSC Cells. To decipher the potential role of miR-2355-5p in HNSC cells, candidate targets of miR-2355-5p were explored using the ENCORI database. A venn diagram demonstrating the overlaps of the microT predicted, miRmap predicted, and negative expression correlated targets with two common genes (NISCH and CBX5) is identified (Figure 2(a)). The relationship between the expression of each gene and OS for TCGA-HNSC patients was assessed through a univariate Cox regression model. NISCH expression was associated with the OS of HNSC patients (Figure 2(a)), and consequently selected as the target for downstream validation. To verify the interaction between miR-2355-5p and NISCH, we first investigated the expression pattern of NISCH in HNSC. We found that NISCH was significantly downregulated in HNSC tissues as compared with the normal tissues in the TCGA-HNSC subset (Figure 2(b)) and collected paired samples (Figure 2(c)). Moreover, the Kaplan–Meier survival curve suggests poor OS with low expression of NISCH compared with those in the high NISCH expression population (Figure 2(d)). Negative correlation between the expression of miR-2355-5p and NISCH was validated in the TCGA-HNSC subset (Figure 2(e)). Luciferase reporter assay and RNA pulldown were performed to further investigate the interaction between miR-2355-5p and NISCH. Transfection with miR-2355-5p mimics significantly decreased the luciferase activity of the NISCH 3′-UTR wildtype reporter

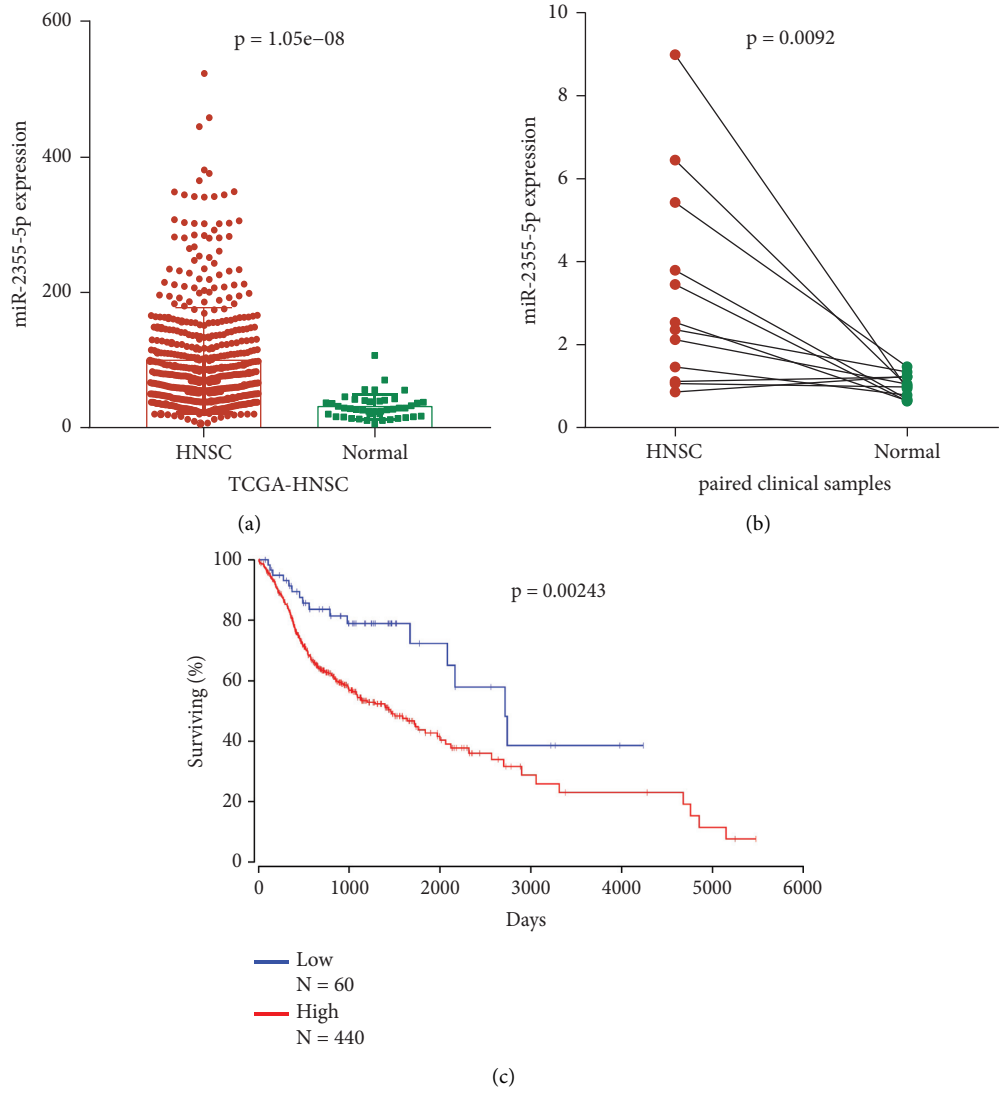

Figure 1: Expression and prognostic value of miR-2355-5p in HNSC. (a) The level of miR-2355-5p in HNSC and normal tissues in the TCGA dataset. (b) Comparison of miR-2355-5p expression in 12 paired samples collected from 12 HNSC patients. (c) Kaplan–Meier plots for overall survival (OS) in TCGA-HNSC patients, grouped by low and high expression of miR-2355-5p. *p* values were obtained using the log-rank test.

gene, but had no effect on that of the NISCH 3′-UTR mutated reporter gene (Figure 3(a)). These results suggest that miR-2355-5p inhibited NISCH expression dependent on binding sequence within 3′-UTR. Furthermore, the mutation of NISCH 3′-UTR significantly decreased the abundance of miR-2355-5p captured by NISCH probes (Figure 3(b), right panel), further validating the binding interaction between miR-2355-5p and NISCH.

3.3. miR-2355-5p Promoted Cell Growth of HNSC Cells. Because miR-2355b-5p was significantly upregulated in HNSC, we evaluated the effect of miR-2355-5p on cell proliferation in CAL27 and SCC25 cells. As indicated in Figure 4(a), miR-2355-5p expression was regulated by transfection with miR-2355-5p mimics and inhibitors in CAL27 and SCC25 cells. Transfection of the miR-2355-5p inhibitor obviously suppressed the growth of HNSC cells, whereas transfection of the inhibitor enhanced their growth (Figure 4(b)). We further examined the effects of miR-2355-5p on cell cycle modulation. Compared with the control, the miR-2355-5p inhibitor caused cell cycle arrest at the G1-phase, as well as restrained cell transit to the S phase (Figure 4(c)). As shown in Edu staining assays, miR-2355-5p significantly increased the proliferating cells (Figure 4(d)), indicating the promotion roles of miR-2355-5p on cell proliferation. Subsequently, the expression of NISCH and cell cycle-related proteins, including CDK1 and p-Rb^{Ser807}, was detected by the western blot assay. Our results showed that miR-2355-5p decreased NISCH expression, while it augmented the protein levels of cyclin D1 and p-Rb^{Ser807}, the indicators of cell cycle arrest (Figure 4(e)). Collectively, these findings suggest that miR-2355-5p inhibits HNSC cell proliferation by arresting the cells at G1/S transition.

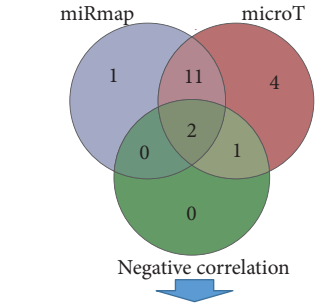

Genes	Cox Coefficient	p value
NISCH	−0.159	2.80e−02
CBX5	−0.122	9.10e−02

(a)

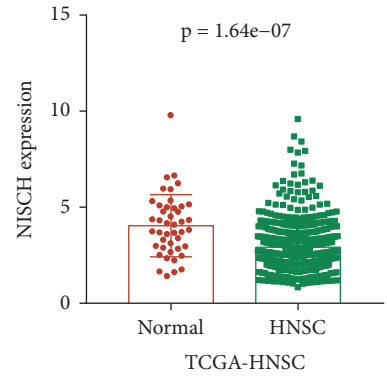

(b)

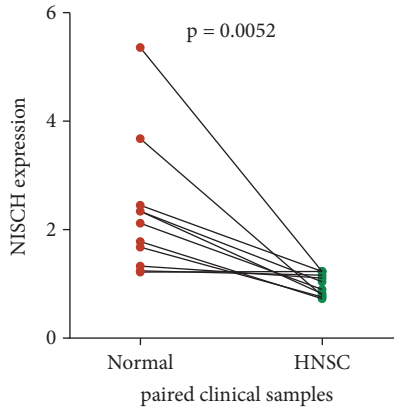

(c)

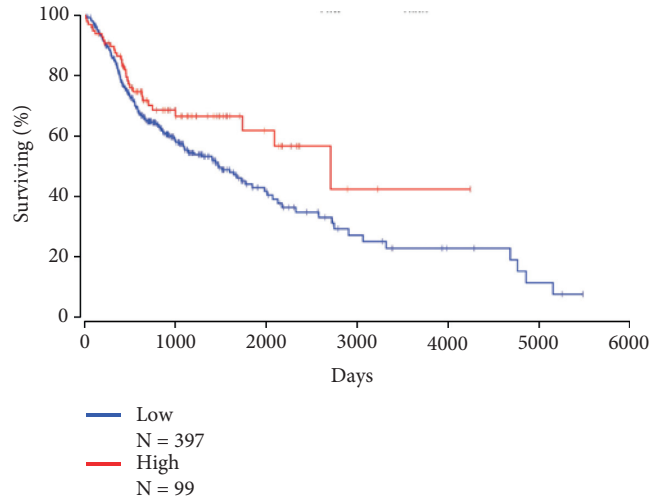

(d)

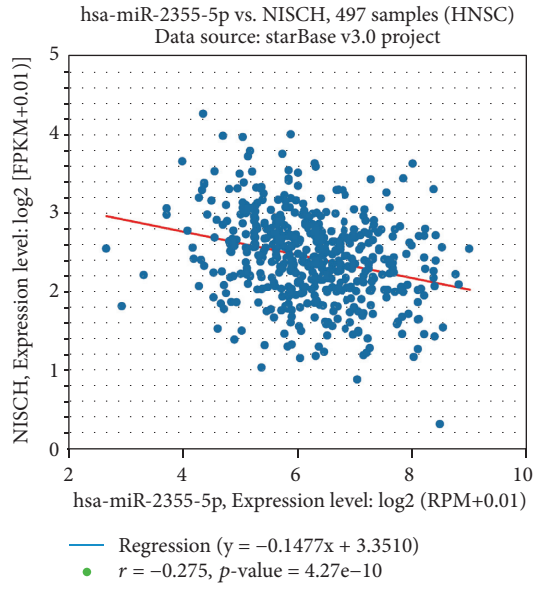

(e)

Figure 2: Expression and prognostic value of NISCH in HNSC. (a) Screening for candidate targets of miR-2355-5p. (b) The level of NISCH in HNSC tissues in the TCGA dataset compared with normal tissues. (c) Comparison of NISCH expression in 12 paired samples collected from HNSC patients. (d) Kaplan–Meier plots for overall survival (OS) in TCGA-HNSC patients, grouped by low and high expression of NISCH. *p* values were obtained using the log-rank test. (e) Pearson correlation analysis shows a negative correlation between miR-2355-5p and NISCH mRNA levels in the TCGA-HNSC subset ($n = 497$).

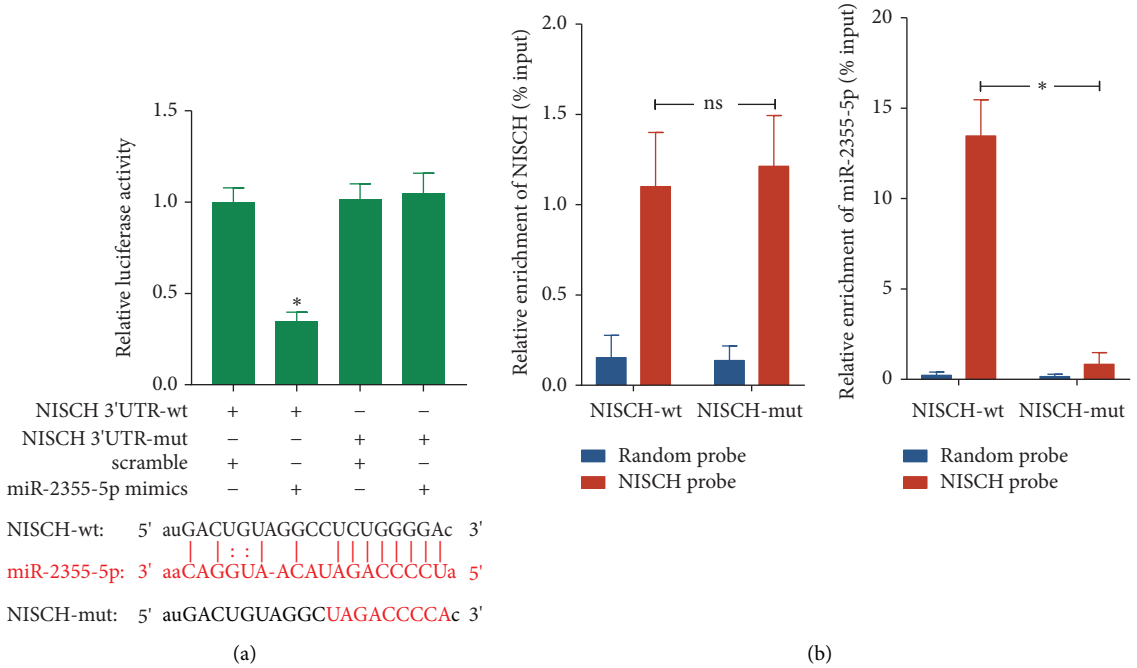

Figure 3: miR-2355-5p repressed NISCH expression by binding to its 3′-UTR. (a) Effects of miR-2355-5p on the luciferase activity of the reporter gene inserted downstream of the wildtype and mutated NISCH 3′-UTR in CAL27 cells. The sequence of the miR-2355-5p binding site within the 3′-UTR of NISCH and its corresponding mutation were indicated. (b) RNA pulldown assay was performed in CAL27 cells transfected with wildtype and mutated NISCH, followed by qRT-PCR to detect the abundance of NISCH and miR-2355-5p. Data are presented as the mean ± standard deviation (SD). ns: not significant; * $p < 0.05$.

3.4. miR-2355-5p Promoted Cell Cycle Progression via Inhibiting NISCH in HNSC Cells. To detect the specific role of the miR-2355-5p/NISCH axis in HNSC, we cotransfected miR-2355-5p inhibitor and si-NISCH into CAL27 and SCC25 cells. The results of CCK-8 and EdU staining assay indicated that the NISCH knockdown attenuated the suppressive effect of miR-2355-5p inhibitor on cell proliferation (Figures 5(a) and 5(b)). Moreover, Western blot revealed that transfection of si-NISCH could downregulate NISCH expression in HNSC cells and weaken the suppressive effect of the miR-2355-5p inhibitor on the protein level of cell cycle-related genes (Figure 5(c)). These results highlighted that the miR-2355-5p/NISCH axis is involved in modulating the cell cycle progression of HNSC cells (Figure 6).

4. Discussion

Although the detection and treatment for HNSC have improved in the last decades, the outcome of HNSC patients remains unsatisfactory in the recent years [29]. In the present study, we found that the dysfunction of the miR-2355-5p/NISCH axis was involved in the promotion of cell cycle progression and was significantly associated with OS in HNSC patients. Moreover, NISCH was the direct target of miR-2355-5p in HNSC.

Cell cycle control provides cancer cells with growth advantages. In normal cells, cellular growth and proliferation are stringently regulated, while derangements of the cell cycle lead to uncontrolled proliferation in cancer cells. Thus, key genes in cell cycle regulation can be investigated as a promising therapeutic target for cancer treatment [30]. Recently, accumulating evidence has indicated the involvement of miRNAs in cell cycle regulation in cancer [31, 32]. Notably, the ceRNA hypothesis sparked a miRNA-mediated mechanism [33] in which miRNA acts as the key modulator linking competing endogenous RNAs, including long noncoding RNA (lncRNA), circular RNA (circRNA), pseudogenes, and protein-coding genes [34–36]. As reported, miR-2355-5p inhibits the occurrence of bladder cancer via regulating DDX11-AS1 and LAMB3 expressions [12]. In chondrosarcoma cells, miR-2355-5p were sponged by exosomal RAMP2-AS1 to promote VEGFR2-mediated angiogenesis [13]. These results suggested the suppressive roles of miR-2355-5p in some cancer types. Unlike them, Zhang's study indicated that the WDFY3-AS2/miR-2355-5p/SOCS2 axis suppresses cell proliferation in oesophageal squamous cell carcinoma, which is consistent with our findings. Notably, Fekete and his colleagues revealed that high miR-2355 expression is correlated with chemoresistance against platinum-based therapy in squamous cell carcinomas [16]. Together with our findings, we speculate that miR-2355-5p provides cells in squamous cell carcinoma with growth advantages and other malignant phenotypes, while it may differ in other pathological types of cancer. Furthermore, we identified NISCH, a promising tumor suppressor gene, as a novel target of miR-2355-5p in HNSC. The expression of NISCH is closely related to tumorigenesis, progression, and poor prognosis in cancers, including breast, lungs, and ovarian cancers [22, 24, 37, 38]. A series of publications reported that NISCH was a tumor-suppressive

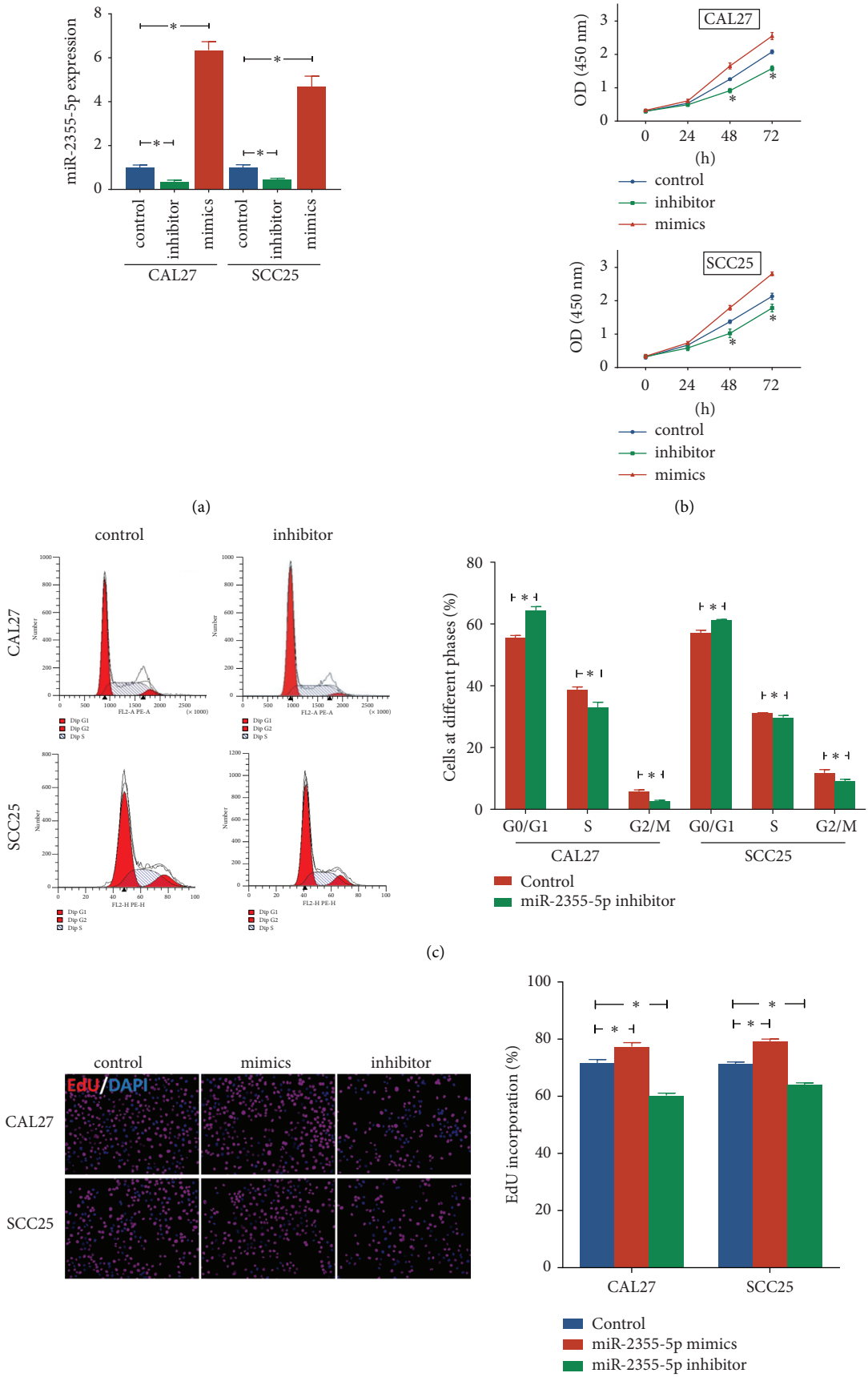

Figure 4: Continued.

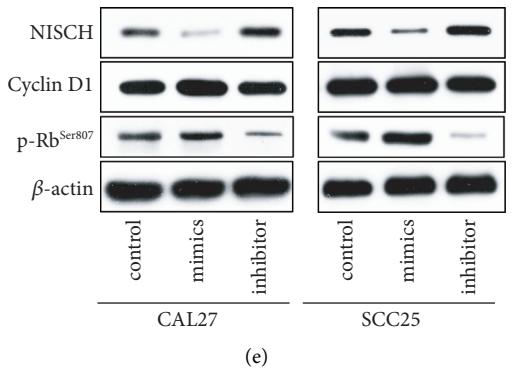

(e)

Figure 4: Effect of miR-2355-5p on cell cycle progression in CAL27 and SCC25 cells. (a) Effects of miR-2355-5p mimics and inhibitor on miR-2355-5p expression in CAL27 and SCC25 cells. (b) The viability of each group of cells was detected by the CCK-8 assay. (c) For each group, cell cycle distribution was detected by flow cytometry analysis. (d) EdU staining (red) was performed to check the proliferating cells. Cell nuclei were stained with DAPI (blue). (e) Levels of NISCH, cyclin D1, and p-Rb^{Ser807} were detected by western blotting analysis in each group, with β-actin as the reference protein. * $p < 0.05$.

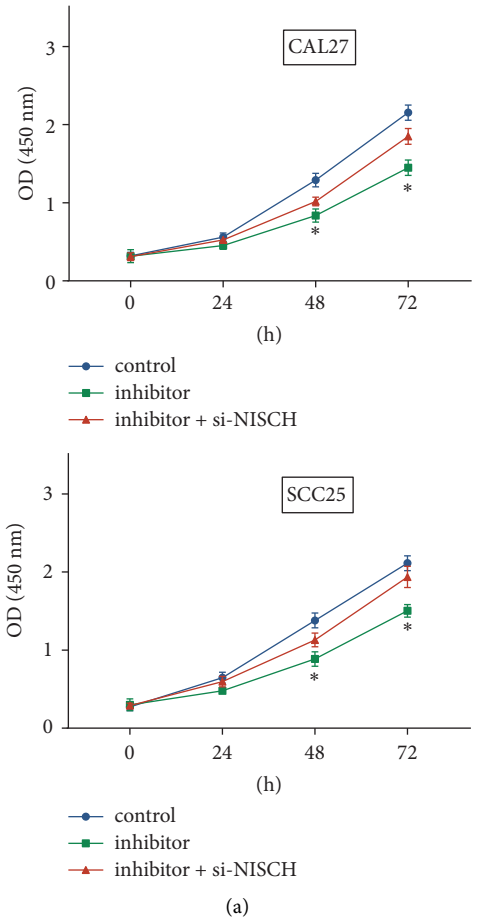

(a)

Figure 5: Continued.

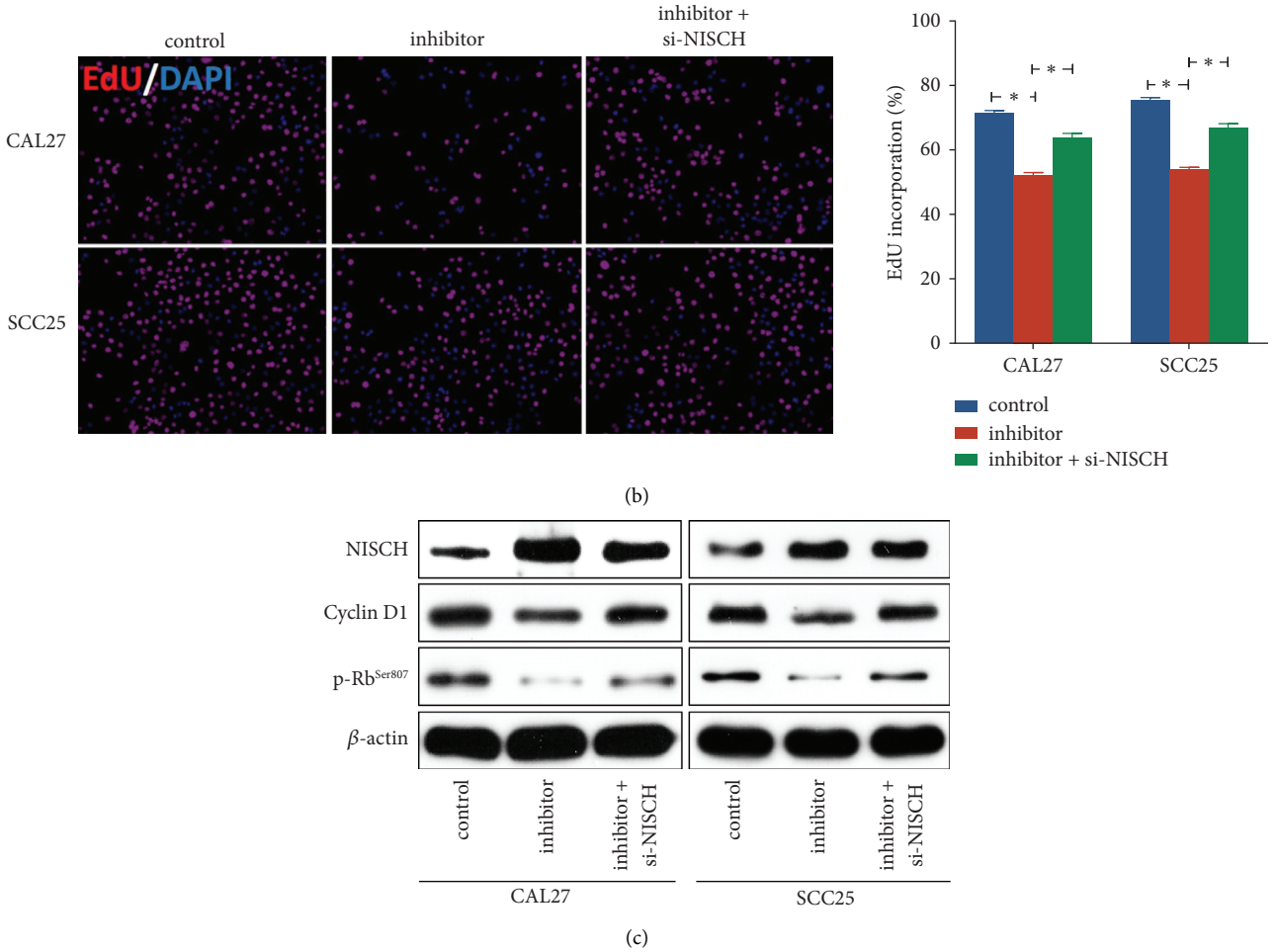

Figure 5: NISCH knockdown attenuates the promotion effects of miR-2355-5p on HNSC cell proliferation. (a) The viability of each group of cells was detected by the CCK-8 assay. (b) EdU staining (red) was performed to check the proliferating cells in each group. Cell nuclei were stained with DAPI (blue). (c) Western blot analysis of the impact of si-NISCH on NISCH, cCyclinD1, and p-Rb^{Ser807} expression. Data are presented as the mean ± SD.

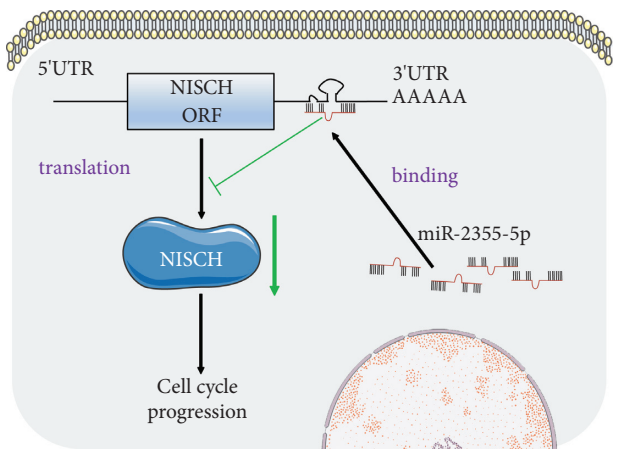

Figure 6: Schematic diagram of the miR-2355-5p/NISCH axis involved in cell proliferation of HNSC. miR-2355-5p promoted cell cycle progression by binding to the 3′-UTR of NISCH in HNSC cells.

factor in breast cancer, and NISCH-expressing cells delivered exosomes that suppress breast cancer cell growth and mobility [21, 37, 39, 40]. In ovarian cancer, promoter hypermethylation-induced NISCH silence-promoted cell cycle progression through the focal adhesion kinase (FAK) signal [22]. Besides, a previous study indicated that tizanidine hydrochloride inhibited A549 cell proliferation and mobility via upregulating the NISCH expression [24]. All the aforementioned results support the results of our study. To further validate the roles of the miR-2355-5p/NISCH axis in HNSC, we performed rescue experiments, which confirmed that miR-2355-5p-promoted cell cycle progression by targeting NISCH in CAL27 and SCC25 cells.

5. Conclusions

Altogether, we have revealed a novel miR-2355-5p/NISCH axis and elaborated its involvement in cell cycle regulation in HNSC. Our findings provide novel insights into future understanding of the molecular mechanisms of cell cycle progression in HNSC.

Data Availability

The datasets analyzed during the current study are available in the TCGA (https://cancergenome.nih.gov) repository. TCGA allows researchers to download relevant data for free for research and publish relevant articles.

Ethical Approval

The present study was approved by the ethics committee of Hunan Cancer Hospital (KYJJ-2020-222), Changsha, China.

Consent

Not applicable.

Conflicts of Interest

The authors declare that they have no conflicts of interest.

Authors' Contributions

Y Long, HZ, WX, Y Liu, and XZ conceived and designed the study; HZ, SL, JD, and ZL collected and prepared the samples; HZ, WX, Y Liu, BZ, SL, XS, MP, QG, CL, and HR performed experiments and data analyses; and Y Long, HZ, and Y Liu wrote the manuscript. All authors reviewed the manuscript and approved the final version. Hailin Zhang, Wei Xie, and Ying Liu contributed equally to this work.

Acknowledgments

The present study was supported in part by the National Natural Science Foundation of China (Grant nos. 81703005 and 81902794), the Natural Science Foundation of Hunan Province (Grant nos. 2017JJ3195, 2018JJ3317, and 2021JJ30427), the Hunan Provincial Science and Technology Department (Grant nos. 2018SK2120, 2018SK2122, 2018SK50907, and 2018SK7005), the Scientific Research Project of Hunan Provincial Health Commission (Grant nos. B2013-097, B2019092, C2019080, 20201650, 20201653, and 202102082037), Changsha Science and Technology Bureau Foundation (Grant nos. kq1706044 and kq1901074), and the Key Clinical Specialty Construction Project (Head & Neck Surgery) of the Provincial Health Commission of Hunan Province. We acknowledge the TCGA database for providing their platforms and contributors for uploading their meaningful datasets.

References

[1] F. Bray, J. Ferlay, I. Soerjomataram, R. L. Siegel, L. A. Torre, and A. Jemal, "Global cancer statistics 2018: GLOBOCAN estimates of incidence and mortality worldwide for 36 cancers in 185 countries," *CA: A Cancer Journal for Clinicians*, vol. 68, no. 6, pp. 394–424, 2018.

[2] K. D. Miller, L. Nogueira, A. B. Mariotto et al., "Cancer treatment and survivorship statistics, 2019," *CA: A Cancer Journal for Clinicians*, vol. 69, no. 5, pp. 363–385, 2019.

[3] A. Gulland, "Oral cancer rates rise by two thirds," *BMJ*, vol. 355, p. i6369, 2016.

[4] L. Jansen, N. Buttmann-Schweiger, S. Listl et al., "Differences in incidence and survival of oral cavity and pharyngeal cancers between Germany and the United States depend on the HPV-association of the cancer site," *Oral Oncology*, vol. 76, pp. 8–15, 2018.

[5] A. B. Pardee and C. J. Li, "Two controls of cell proliferation underlie cancer relapse," *Journal of Cellular Physiology*, vol. 233, no. 11, pp. 8437–8440, 2018.

[6] S. Wang, Y. Zhang, Y. Liu et al., "Inhibition of CSRP2 promotes leukemia cell proliferation and correlates with relapse in adults with acute myeloid leukemia," *OncoTargets and Therapy*, vol. 13, pp. 12549–12560, 2020.

[7] A. Eulalio, E. Huntzinger, and E. Izaurralde, "Getting to the root of miRNA-mediated gene silencing," *Cell*, vol. 132, no. 1, pp. 9–14, 2008.

[8] J. Hausser and M. Zavolan, "Identification and consequences of miRNA-target interactions—beyond repression of gene expression," *Nature Reviews Genetics*, vol. 15, no. 9, pp. 599–612, 2014.

[9] R. Rupaimoole, G. A. Calin, G. Lopez-Berestein, and A. K. Sood, "miRNA deregulation in cancer cells and the tumor microenvironment," *Cancer Discovery*, vol. 6, no. 3, pp. 235–246, 2016.

[10] L. Yi, Y. Liu, A. Xu et al., "MicroRNA-26b-5p suppresses the proliferation of tongue squamous cell carcinoma via targeting proline rich 11 (PRR11)," *Bioengineered*, vol. 12, no. 1, pp. 5830–5838, 2021.

[11] Y. Cheng, X. Shang, D. Chen, D. Pang, C. Zhao, and X. Xu, "MicroRNA-2355-5p regulates γ-globin expression in human erythroid cells by inhibiting KLF6," *British Journal of Haematology*, vol. 193, no. 2, pp. 401–405, 2021.

[12] D. Chen, J. Chen, J. Gao et al., "LncRNA DDX11-AS1 promotes bladder cancer occurrence via protecting LAMB3 from downregulation by sponging miR-2355-5p," *Cancer Biotherapy and Radiopharmaceuticals*, vol. 35, no. 5, pp. 319–328, 2020.

[13] C. Cheng, Z. Zhang, F. Cheng, and Z. Shao, "Exosomal lncRNA RAMP2-AS1 derived from chondrosarcoma cells promotes angiogenesis through miR-2355-5p/VEGFR2 axis," *OncoTargets and Therapy*, vol. 13, pp. 3291–3301, 2020.

[14] Q. Zhang, F. Guan, T. Fan et al., "LncRNA WDFY3-AS2 suppresses proliferation and invasion in oesophageal squamous cell carcinoma by regulating miR-2355-5p/SOCS2 axis," *Journal of Cellular and Molecular Medicine*, vol. 24, no. 14, pp. 8206–8220, 2020.

[15] L. Hao, Q. Zhang, H.-Y. Qiao et al., "TRIM29 alters bioenergetics of pancreatic cancer cells via cooperation of miR-2355-3p and DDX3X recruitment to AK4 transcript," *Molecular Therapy—Nucleic Acids*, vol. 24, pp. 579–590, 2021.

[16] J. T. Fekete, Á Welker, and B. Győrffy, "miRNA expression signatures of therapy response in squamous cell carcinomas," *Cancers*, vol. 13, no. 1, 2020.

[17] W. Sun, Z. Qiu, W. Huang, and M. Cao, "Gene expression profiles and proteinprotein interaction networks during tongue carcinogenesis in the tumor microenvironment," *Molecular Medicine Reports*, vol. 17, no. 1, pp. 165–171, 2018.

[18] F. Tian, J. Zhao, X. Fan, and Z. Kang, "Weighted gene co-expression network analysis in identification of metastasis-related genes of lung squamous cell carcinoma based on the cancer genome atlas database," *Journal of Thoracic Disease*, vol. 9, no. 1, pp. 42–53, 2017.

[19] P. Dai, Y. He, G. Luo et al., "Screening candidate microRNA-mRNA network for predicting the response to chemo-resistance in osteosarcoma by bioinformatics analysis,"

Journal of Cellular Biochemistry, vol. 120, no. 10, pp. 16798–16810, 2019.

[20] Y. Zhao, J. Huang, and J. Chen, "The integration of differentially expressed genes based on multiple microarray datasets for prediction of the prognosis in oral squamous cell carcinoma," *Bioengineered*, vol. 12, no. 1, pp. 3309–3321, 2021.

[21] S. Baranwal, Y. Wang, R. Rathinam et al., "Molecular characterization of the tumor-suppressive function of nischarin in breast cancer," *Journal of the National Cancer Institute*, vol. 103, no. 20, pp. 1513–1528, 2011.

[22] J. Li, X. He, R. Dong, Y. Wang, J. Yu, and H. Qiu, "Frequent loss of NISCH promotes tumor proliferation and invasion in ovarian cancer via inhibiting the FAK signal pathway," *Molecular Cancer Therapeutics*, vol. 14, no. 5, pp. 1202–1212, 2015.

[23] S. Dong, B. Ruiz-Calderon, R. Rathinam, S. Eastlack, M. Maziveyi, and S. K. Alahari, "Knockout model reveals the role of nischarin in mammary gland development, breast tumorigenesis and response to metformin treatment," *International Journal of Cancer*, vol. 146, no. 9, pp. 2576–2587, 2020.

[24] L. Zhao, G. Zhao, and Q. Xue, "Tizanidine (hydrochloride) inhibits A549 lung cancer cell proliferation and motility through regulating nischarin," *OncoTargets and Therapy*, vol. 13, pp. 291–298, 2020.

[25] Cancer Genome Atlas Research Network, J. N. Weinstein, E. A. Collisson et al., "The cancer genome atlas pan-cancer analysis project," *Nature Genetics*, vol. 45, no. 10, pp. 1113–1120, 2013.

[26] J. H. Li, S. Liu, H. Zhou, L. H. Qu, and J. H. Yang, "StarBase v2.0: decoding miRNA-ceRNA, miRNA-ncRNA and protein-RNA interaction networks from large-scale CLIP-Seq data," *Nucleic Acids Research*, vol. 42, pp. D92–D97, 2014.

[27] J. H. Yang, J. H. Li, P. Shao, H. Zhou, Y. Q. Chen, and L. H. Qu, "starBase: a database for exploring microRNA-mRNA interaction maps from argonaute CLIP-Seq and degradome-Seq data," *Nucleic Acids Research*, vol. 39, pp. D202–D209, 2011.

[28] J. Anaya, "OncoLnc: linking TCGA survival data to mRNAs, miRNAs, and lncRNAs," *PeerJ Computer Science*, vol. 2, p. e67, 2016.

[29] D. Y. Lee, J. Abraham, E. Ross et al., "Rapid recurrence in head and neck cancer: underappreciated problem with poor outcome," *Head & Neck*, vol. 43, no. 1, pp. 212–222, 2021.

[30] K. Vermeulen, D. R. Van Bockstaele, and Z. N. Berneman, "The cell cycle: a review of regulation, deregulation and therapeutic targets in cancer," *Cell Proliferation*, vol. 36, no. 3, pp. 131–149, 2003.

[31] L. Wang, S. Ge, and F. Zhou, "MicroRNA-487a-3p inhibits the growth and invasiveness of oral squamous cell carcinoma by targeting PPM1A," *Bioengineered*, vol. 12, no. 1, pp. 937–947, 2021.

[32] H. Liu, Z. Chi, H. Jin, and W. Yang, "MicroRNA miR-188-5p as a mediator of long non-coding RNA MALAT1 regulates cell proliferation and apoptosis in multiple myeloma," *Bioengineered*, vol. 12, no. 1, pp. 1611–1626, 2021.

[33] L. Salmena, L. Poliseno, Y. Tay, L. Kats, and P. P. Pandolfi, "A ceRNA hypothesis: the rosetta stone of a hidden RNA language?" *Cell*, vol. 146, no. 3, pp. 353–358, 2011.

[34] L. Wang, J. Yi, L.-Y. Lu et al., "Estrogen-induced circRNA, circPGR, functions as a ceRNA to promote estrogen receptor-positive breast cancer cell growth by regulating cell cycle-related genes," *Theranostics*, vol. 11, no. 4, pp. 1732–1752, 2021.

[35] H. Zhang, H. Zhang, X. Li, S. Huang, Q. Guo, and D. Geng, "LINC01089 functions as a ceRNA for miR-152-3p to inhibit non-small lung cancer progression through regulating PTEN," *Cancer Cell International*, vol. 21, no. 1, p. 143, 2021.

[36] M. Vitiello, M. Evangelista, Y. Zhang, L. Salmena, P. P. Pandolfi, and L. Poliseno, "PTENP1 is a ceRNA for PTEN: it's CRISPR clear," *Journal of Hematology & Oncology*, vol. 13, no. 1, p. 73, 2020.

[37] M. Maziveyi and S. K. Alahari, "Breast cancer tumor suppressors: a special emphasis on novel protein nischarin," *Cancer Research*, vol. 75, no. 20, pp. 4252–4259, 2015.

[38] C. Chang, W. Wei, D. Han et al., "Expression of nischarin negatively correlates with estrogen receptor and alters apoptosis, migration and invasion in human breast cancer," *Biochemical and Biophysical Research Communications*, vol. 484, no. 3, pp. 536–542, 2017.

[39] M. Maziveyi, S. Dong, S. Baranwal et al., "Exosomes from nischarin-expressing cells reduce breast cancer cell motility and tumor growth," *Cancer Research*, vol. 79, no. 9, pp. 2152–2166, 2019.

[40] K. M. McAndrews and R. Kalluri, "Nischarin regulates secretion of exosomes and cancer progression," *Cancer Research*, vol. 79, no. 9, pp. 2099–2101, 2019.